IOPscience iopscience.iop.org

Home Search Collections Journals About Contact us My IOPscience

The effect of oxygen deficiency on the structural phase transition and electronic and magnetic properties of the spinel $LiMn_2O_{4-\delta}$

This article has been downloaded from IOPscience. Please scroll down to see the full text article.

1997 J. Phys.: Condens. Matter 9 1729

(http://iopscience.iop.org/0953-8984/9/8/006)

View the table of contents for this issue, or go to the journal homepage for more

Download details:
IP Address: 171.66.16.207
The article was downloaded on 14/05/2010 at 08:10

Please note that terms and conditions apply.

J. Phys.: Condens. Matter **9** (1997) 1729–1741. Printed in the UK PII: S0953-8984(97)76041-7

The effect of oxygen deficiency on the structural phase transition and electronic and magnetic properties of the spinel $LiMn_2O_{4-\delta}$

Jun Sugiyama†, Taroh Atsumi‡, Akihiko Koiwai†, Tsuyoshi Sasaki†, Tatsumi Hioki†, Shoji Noda† and Naoki Kamegashira‡

† Toyota Central Research and Developments Laboratories Inc., 41-1 Yokomichi, Nagakute, Aichi 480-11, Japan

‡ Department of Materials Science, Toyohashi University of Technology, Tempaku-cho, Toyohashi, Aichi 441, Japan

Received 8 July 1996, in final form 7 October 1996

Abstract. The effect of oxygen deficiency on a phase transition from cubic to tetragonal phase has been investigated for the $LiMn_2O_{4-\delta}$ spinels with $\delta = 0$–0.1 by measurements of differential scanning calorimetry (DSC), magnetic susceptibility (χ), ^{7}Li nuclear magnetic resonance (^{7}Li NMR) and electronic resistivity (ρ). According to the DSC measurements, the transition temperature for a stoichiometric compound (T_C) is determined to be 245 ± 1 K. As δ increases from zero to 0.066, the magnitude of T_C is found to decrease by about 4 K; then, the magnitude of T_C increases by about 41 K with further increase of δ up to 0.10; thus, the T_C-versus-δ curve exhibits a broad minimum at around $\delta = 0.05$. This relationship between T_C and δ is also observed by the measurements of χ, ^{7}Li NMR and ρ. The dependence of T_C on δ is considered to be a result of a competition between a decrease in the average valence of Mn ions and a dilution of the nearest-neighbour interaction between Mn ions. Both effects are caused by the oxygen deficiency; the former raises T_C, whereas the latter reduces it.

1. Introduction

The spinel compound $LiMn_2O_4$ has attracted much attention as a cathode material for rechargeable lithium batteries [1–3] due to a reversible intercalation of Li ions into $LiMn_2O_4$ [4, 5]. At ambient temperature, the crystal structure of $LiMn_2O_4$ belongs to the $Fd3m$ space group [6] of a cubic system; the oxygen ions form a cubic closed-packed lattice with the Li and Mn ions occupying the tetrahedrally and octahedrally coordinate interstices, respectively. According to recent reports [7, 8], $LiMn_2O_4$ undergoes a structural phase transition from the cubic phase to a tetragonal $I4_1/amd$ phase with lowering temperature. The transition temperature (T_C) was reported at around 280 K by a differential scanning calorimetry (DSC) analysis [7] and at around 230 K by an elastic measurement [8]. Since the transition occurs in the vicinity of ambient temperature, the performance of the lithium batteries using $LiMn_2O_4$ would strongly depend on temperature. Actually, the capacity of the lithium battery, in which $LiMn_2O_4$ was used as a cathode and Li metal as an anode, is known to reduce with lowering temperature [9]. Nevertheless, to the authors' knowledge, there is a limited data concerning the changes in physical properties during the phase transition for $LiMn_2O_4$; at present, even the magnitude of T_C is not clear, as mentioned above.

0953-8984/97/081729+13$19.50 © 1997 IOP Publishing Ltd

Furthermore, $LiMn_2O_4$ has been found to release oxygen in a reducing atmosphere at temperatures above 873 K [10–12]. For the oxygen deficient $LiMn_2O_{4-\delta}$ spinels, electronic and magnetic structures are expected to be altered due to a change in a valence state of Mn ions and/or a dilution of an superexchange interaction between Mn ions through intervening oxygen. Additionally, for $LiMn_2O_{4-\delta}$, as δ increases from zero, the cubic phase changes into the tetragonal $I4_1/amd$ phase at around $\delta = 0.07$ even at ambient temperature [12]. Therefore, not only electronic and magnetic properties but also the magnitude of T_C would depend on δ. As a result, the performance of the lithium batteries is considered to be a function of both temperature and δ.

Here, we report the effect of δ on the structural phase transition and the electronic and magnetic properties for $LiMn_2O_{4-\delta}$. Also, we report the dependence of the magnitude of T_C on δ and discuss the origin of this dependence using the model proposed for mixed spinels containing Jahn–Teller ions at the octahedral site.

2. Experimental details

Powder samples of $LiMn_2O_{4-\delta}$ with $\delta \leqslant 0.1$ were synthesized by a solid state reaction technique using reagent-grade Li_2CO_3 and MnO_2 powders. The powders were thoroughly mixed by a planetary ball mill using ethanol as solvent. After drying, the mixture was pressed into a pellet with 30 mm diameter and $\sim$ 5 mm thick. The pellet was calcined three times at 1073 K for 8 h in air. In order to control the oxygen content of the sample, the calcined powder was annealed at temperatures between 873 and 1023 K for 24 h in an O_2/Ar gas mixture flow. Then, the annealed powder was cooled to 273 K in a few seconds. Oxygen nonstoichiometry δ was measured using a thermogravimetric technique and an inductively coupled plasma spectrometry together with a chemical titration analysis. The measurement accuracy of δ was estimated to be ± 0.005. Powder x-ray diffraction analyses indicated that the samples with $\delta \leqslant 0.079$ were of single phase of a cubic spinel structure with the lattice parameter $a \sim 0.824$ nm, while the sample with $\delta = 0.10$ consisted of the cubic spinel phase and a tetragonal spinel phase. The preparation and characterization of the $LiMn_2O_{4-\delta}$ samples are reported in detail elsewhere [12].

A differential scanning calorimetry (DSC) analysis was carried out using a power compensation method (Perkin–Elmer, DSC-7). Magnetic susceptibility (χ) was measured using a superconducting quantum interference device (SQUID) magnetometer (Quantum Design, MPMS). The data were measured in a field-cool mode with a magnetic field of $H = 1$ T. A nuclear magnetic resonance (NMR) measurement was performed in a spin echo pulse sequence mode using a Fourier-transform NMR spectrometer (Bruker, MSL-300) under a magnetic field of $H = 7$ T. Static powder was used for the measurement to control the temperature of the sample accurately. The resonance frequency for free ^{7}Li nuclei was determined from the ^{7}Li-NMR line of 1 mol dm^{-3} LiOH aqueous solution. Each measurement accuracy of the shift and the full width at half maximum of the ^{7}Li-NMR line was estimated to be ± 4 ppm.

Electrical resistivity (ρ) of the sample was measured by a dc four-probe method using a sintered disc of the $LiMn_2O_{4-\delta}$ sample; the calcined powder was pressed into a disc with 10 mm diameter and $\sim$ 2 mm thick, and then the disc was annealed at 1023 K in air. The oxygen content of the disc-shaped sample was controlled and checked using a similar method as described for the powder samples of $LiMn_2O_{4-\delta}$.

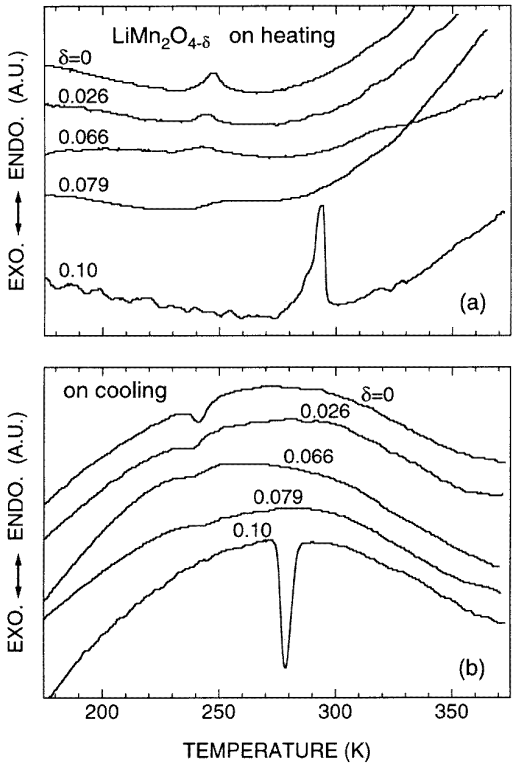

Figure 1. DSC curves for $LiMn_2O_{4-\delta}$ with $\delta = 0$, 0.026, 0.066, 0.079 and 0.10 in the temperature range between 175 and 375 K: data obtained (a) on heating with a rate of 5 K min^{-1} and (b) on cooling with a rate of 5 K min^{-1}.

3. Results

3.1. DSC analysis

Figure 1 shows the DSC curves for the $LiMn_2O_{4-\delta}$ samples with $\delta = 0$, 0.026, 0.066, 0.079 and 0.10 in the temperature range between 175 and 375 K. For the $LiMn_2O_4$ sample, as temperature rises from 113 K with a rate of 5 K min^{-1}, the DSC curve exhibits an endothermic peak at 247 ± 1 K (see figure 1(a)). In contrast, an exothermic peak was observed at 242 ± 0.8 K in the DSC curve measured on cooling with a rate of 5 K min^{-1} (see figure 1(b)). Both peaks are attributed to the phase transition between cubic and tetragonal phases; thus, the magnitude of the transition temperature (T_C) for $LiMn_2O_4$ was determined to be 245 ± 1 K; since the difference between the magnitudes of T_C observed on cooling and on heating (ΔT_C) was 5 ± 2 K, this phase transition was thought to be discontinuous, as had been reported [7]. For the samples with $\delta = 0.026$–0.10, the magnitudes of T_C and ΔT_C were estimated to be 241 ± 1 and 6 ± 2 K for $LiMn_2O_{3.974}$, 242 ± 2 and 3 ± 3 K for $LiMn_2O_{3.934}$, 249 ± 2 and 8 ± 3 K for $LiMn_2O_{3.921}$ and 286 ± 1 and 14 ± 1 K for $LiMn_2O_{3.90}$, respectively. Figure 2(a) shows the relationship between the magnitude of T_C and δ. As δ increased from 0 to 0.066, the magnitude of T_C was found to decrease by about 4 K; then,

the magnitude of T_C increased rapidly with further increase of δ up to 0.10. As a result, the T_C-versus-δ curve seems to exhibit a broad minimum at around $\delta = 0.05$. In addition, as δ increased from 0 to 0.079, the intensity and the width of the DSC peak decreased and extended, while, for the $LiMn_2O_{3.90}$ sample, the DSC peak at T_C looked sharp compared with those for the other samples (see figure 1). Figure 2(b) shows the latent heat ΔH of the phase transition at T_C as a function of δ; here, ΔH was estimated from the area of the DSC peak, and the error bars represent the difference between ΔH obtained on heating and on cooling. As δ increased from 0 to 0.079, ΔH seemed to decrease slightly, and then ΔH increased rapidly with further increase of δ. The values of ΔH were considerably smaller than those for the spinels, which have Mn^{3+} ions at the octahedral sites and undergo a structural phase transition from cubic to tetragonal phases, i.e., $\Delta H \sim$ 21 kJ mol^{-1} for Mn_3O_4 and 14.7 kJ mol^{-1} for $MgMn_2O_4$ [13]. This is probably due to a small distortion of the tetragonal phase (c/a) of $LiMn_2O_4$ compared with those of Mn_3O_4 and $MgMn_2O_4$; that is, the value of c/a of $LiMn_2O_4$ was 1.011 [7] near T_C, while those were 1.13 and 1.16 for Mn_3O_4 and $MgMn_2O_4$ [13], respectively.

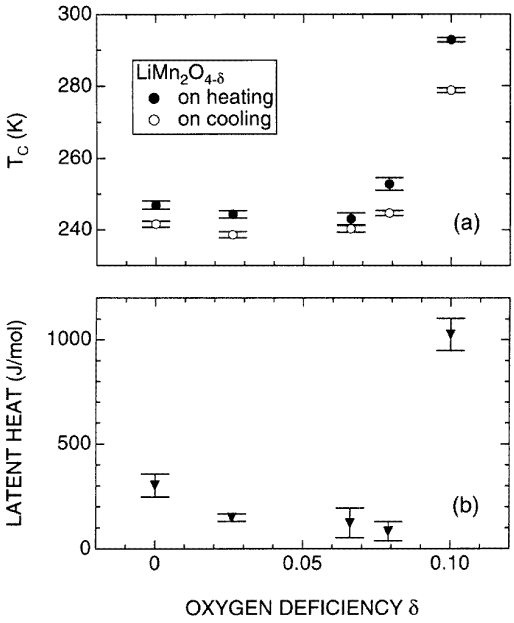

Figure 2. (a) The relationship between the phase transition temperature T_C and oxygen nonstoichiometry δ, in which open circles represent data obtained on cooling and solid circles twice on heating; and (b) the relationship between the latent heat ΔH and δ; error bars represent the difference between the values of ΔH estimated using the data obtained on cooling and on heating.

3.2. Magnetic susceptibility

Figure 3(a) and (b) shows the temperature dependences of magnetic susceptibility χ and $1/\chi$ respectively for the $LiMn_2O_{4-\delta}$ samples with $\delta = 0$–0.10. For the samples with $\delta = 0$–0.079, as the temperature was lowered from 400 K, χ of every sample increased

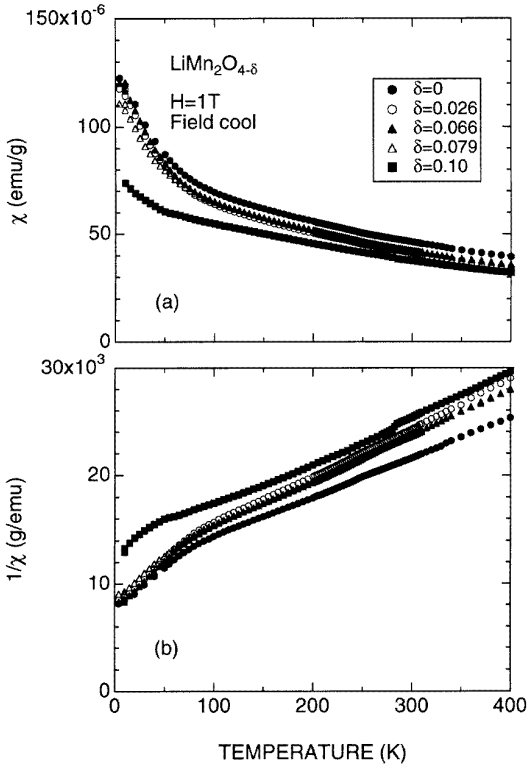

Figure 3. The temperature dependences of (a) magnetic susceptibility χ and (b) $1/\chi$ for $LiMn_2O_{4-\delta}$ with $\delta = 0$–0.10; χ was measured in a field-cool mode under a magnetic field of $H = 1$ T.

monotonically down to around 100 K and then seemed to diverge below 100 K. For the $LiMn_2O_{3.90}$ sample, as the temperature was lowered, χ increased monotonically down to around 10 K, though the slope of χ changed at around 70 K. In addition, the value of χ was found to decrease with increasing δ for the samples with $\delta = 0$–1.0. As seen in figure 3(b), for each of the samples, an approximately linear relationship between $1/\chi$ and temperature was observed in the temperature range between 150 and 400 K. However, at temperatures below 150 K, for the samples with $\delta \leqslant 0.079$, $1/\chi$ of every sample began to deviate from the linear relationship; that is, the slope of $1/\chi$ at temperatures below 150 K was steeper than that above 150 K. This is due to an antiferromagnetic ordering of Mn moments at temperatures below 40 K [14]. On the other hand, for the $LiMn_2O_{3.90}$ sample, the deviation of $1/\chi$ from the linear relationship was found to be positive in the temperature range between 4.2 and 150 K.

Figure 4(a) and (b) shows the temperature dependences of χ and $1/\chi$ respectively in the vicinity of T_C. For the $LiMn_2O_4$ sample, a clear change in the slope was observed at around 250 K in both χ-versus-T and $1/\chi$-versus-T curves. On the other hand, for the $LiMn_2O_{3.90}$ sample, as temperature lowered, a small increase in χ and a small decrease in $1/\chi$ were observed at around 282 K. Although, for the samples with $\delta = 0.026$–0.079, χ of every sample appeared to change slope at around 250 K, it was difficult to determine the

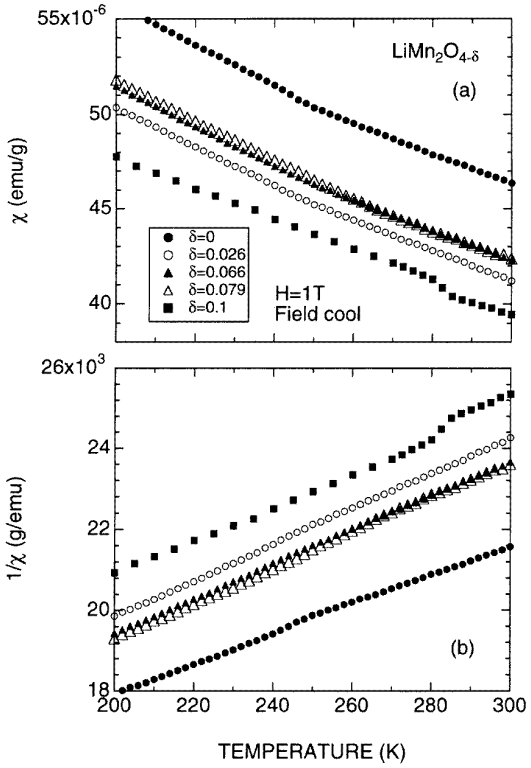

Figure 4. A magnification of the temperature dependences of (a) χ and (b) $1/\chi$ for the $LiMn_2O_{4-\delta}$ samples with $\delta = 0$–0.10.

magnitude of T_C precisely based only on this result. Such small anomalies of χ at T_C have been also reported for $TbVO_4$ and $DyVO_4$ [15], which undergo a structural phase transition caused by the cooperative Jahn–Teller effects.

It should be noted that, for the samples with $\delta = 0$–0.10, the $1/\chi$-versus-T curve of every sample seems to be approximately linear in the temperature range between 150 and 400 K, though the slope of $1/\chi$ changes slightly at T_C. In particular, for the samples with $\delta \leqslant 0.079$, the χ-versus-T curves of every sample seem to be parallel to each other; thus, this indicates that the macroscopic magnetic structure of the sample remains during the phase transition at T_C.

3.3. ^{7}Li NMR

For the samples with $\delta = 0$, 0.026, 0.079 and 0.10, the ^{7}Li NMR lines at temperatures above T_C appeared symmetrical, with no indications of peak split. Figure 5(a)–(d) show the temperature dependence of the shift (K) of the ^{7}Li NMR line for the samples with $\delta = 0$, 0.026, 0.079 and 0.10 respectively. The value of K at ambient temperature for the $LiMn_2O_4$ sample was comparable with the results of the previous NMR studies [16, 17]. At temperatures above T_C, K of every sample increased monotonically with decreasing temperature. Therefore, the local magnetic field at the Li ion increased with decreasing

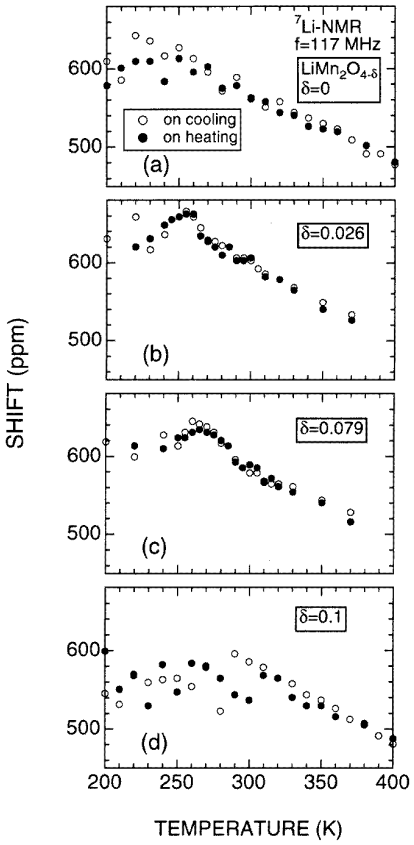

Figure 5. The temperature dependence of the shift K of the ^{7}Li NMR line for (a) $LiMn_2O_4$, (b) $LiMn_2O_{3.974}$, (c) $LiMn_2O_{3.921}$ and (d) $LiMn_2O_{3.90}$; open circles represent data obtained on cooling and solid circles on heating.

temperature. This is in good agreement with the measured χ-versus-T curves. Indeed, a linear relationship between K and χ was obtained at temperatures above T_C, as seen in figure 6(a). Assuming that the temperature dependence of K is responsible for the Mn moment, we can estimate the hyperfine field at the Li ion to be 0.75 ± 0.04, 0.93 ± 0.04, 0.95 ± 0.07 and 1.12 ± 0.03 kOe μ_B for the samples with $\delta = 0$, 0.026, 0.079 and 0.10, respectively. Thus, the hyperfine field at the Li ion increases with increasing δ. This suggests that the microscopic magnetic interaction between the Mn moments would be altered by the oxygen deficiency, probably due to a change in a superexchange interaction between Mn ions through intervening oxygen.

As the temperature was lowered from T_C, for the $LiMn_2O_4$ and $LiMn_2O_{3.90}$ samples, K seemed to roughly level off to a constant value, though the accuracy of the measured K at temperatures below T_C was lower than that above T_C. Additionally, for the $LiMn_2O_{3.90}$ sample, the magnitude of ΔT_C was estimated to be 20–30 K. For the samples with $\delta = 0.026$ and 0.079, K values of both samples changed the sign of the slope from negative to positive at T_C; that is, there existed a peak at T_C in the K-versus-T curve.

Figures 7(a)–(d) shows the full width at half maximum (FWHM) of the ^{7}Li NMR line

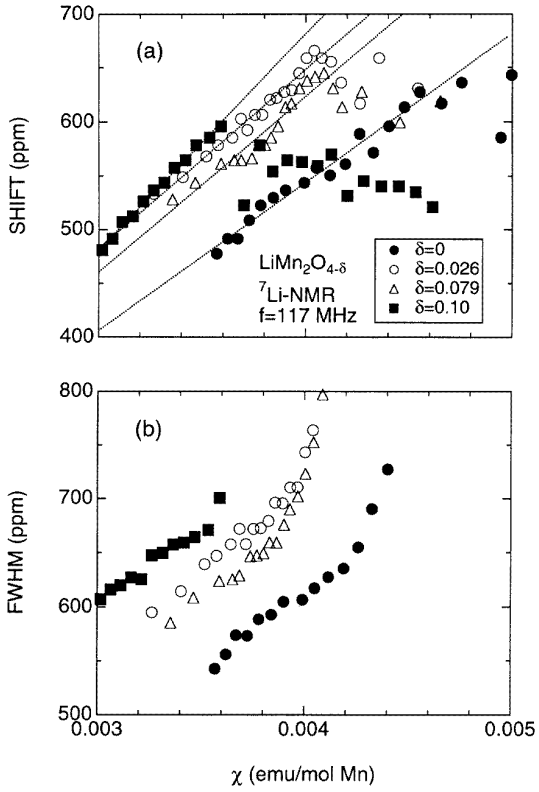

Figure 6. The relationship (a) between K and χ and (b) between the full width at half maximum (FWHM) and χ for $LiMn_2O_{4-\delta}$ with $\delta = 0$–0.10; the four dotted lines in (a) were obtained by fitting the experimental data measured at temperatures above T_C.

as a function of temperature. For the samples with $\delta = 0$–0.10, as the temperature was lowered from 400 K, FWHM of every sample increased monotonically down to T_C, and then FWHM increased rapidly with further lowering of the temperature. This is because, as the temperature was lowered from T_C, a shoulder of the resonance peak on the low-magnetic field side appeared for every sample; the intensity of the shoulder increased with decreasing temperature. Since the FWHM of every sample increases approximately proportionally to χ at temperatures above T_C (see figure 6(b)), FWHM is attributed to the coupling between the Li nuclear magnetic moments and the Mn moments. The difference between the data obtained on heating and on cooling was observed only for the sample with $\delta = 0.10$; the magnitude of ΔT_C was about 20 K.

According to the x-ray diffraction analysis [7], $LiMn_2O_4$ was found to be a mixture of the cubic spinel and the tetragonal spinel phases at temperatures below T_C, while $LiMn_2O_4$ was assigned to be a single phase of the cubic spinel structure at temperatures above T_C. Hence, the change in the slope of FWHM at T_C suggests that there is a marked difference between the dipole fields at the Li sites in the cubic phase (Li(c) site) and in the tetragonal phase (Li(t) site). Furthermore, this result indicates that the temperature dependence of the dipole field at the Li(c) site is different from that at the Li(t) site.

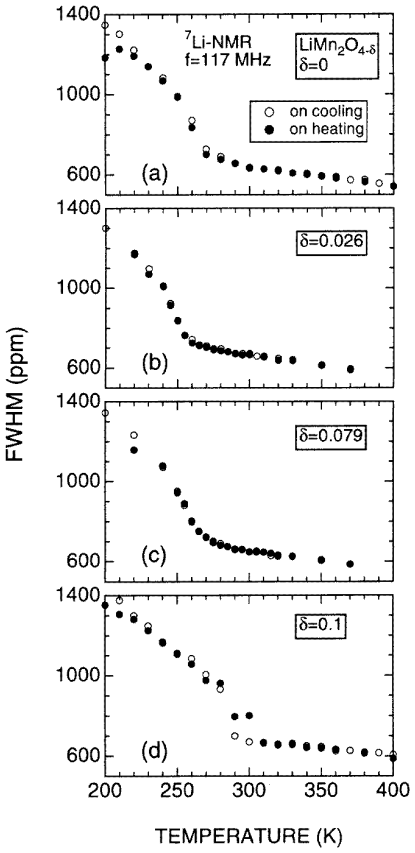

Figure 7. The temperature dependence of FWHM of the ^{7}Li NMR line for (a) $LiMn_2O_4$, (b) $LiMn_2O_{3.974}$, (c) $LiMn_2O_{3.921}$ and (d) $LiMn_2O_{3.90}$; open circles represent data obtained on cooling and solid circles on heating.

3.4. Resistivity

Figure 8 shows the relationship between resistivity (ρ) and reciprocal temperature ($1/T$) for the samples with $\delta = 0$–0.101 in the temperature range between 295 and 225 K obtained on heating. The samples used for the ρ measurement were a different set from those used for the DSC, NMR and χ measurements. As the temperature was raised from 225 K, $\log \rho$ of every sample decreased in proportion to $1/T$ up to T_C, decreased by one order of magnitude around T_C, and then decreased monotonically with decreasing $1/T$. The optimal value of δ, at which T_C exhibits the lowest value, was estimated to be about 0.03. Although the two sets of samples were used for the present work, the relationships between T_C and δ for both sets of samples were consistent with each other.

Finally, figure 9 shows the relationship between $\log(\rho/T^{1.5})$ and $1/T$ for the $LiMn_2O_4$ sample in the temperature range between 1243 and 225 K. A sudden increase in $\log(\rho/T^{1.5})$ around 1200 K is due to a loss of oxygen from the sample. A linear relationship between $\log(\rho/T^{1.5})$ and $1/T$ is observed in the temperature range between T_C and 1200 K, as expected for small polaron formation. The activation energy for electron transfer (E_a) was

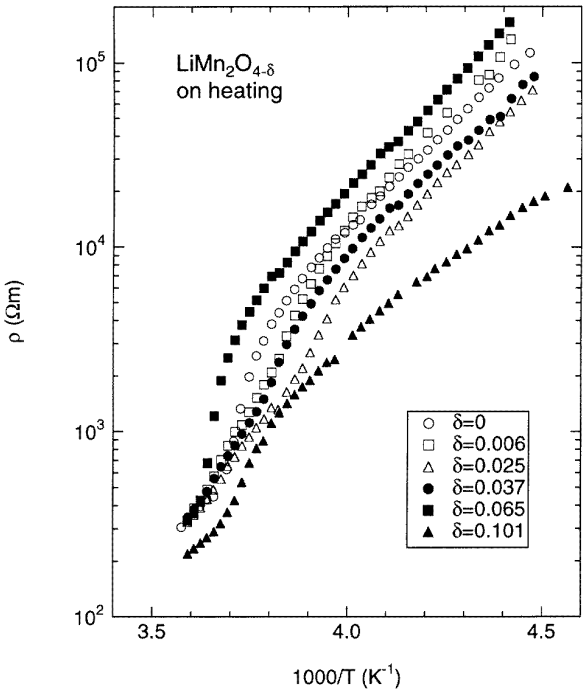

Figure 8. The relationship between resistivity ρ and reciprocal temperature T^{-1} for $LiMn_2O_{4-\delta}$ with $\delta = 0$–0.101.

estimated to be 0.39 eV. This value is comparable with those for the various kinds of spinel-type compound which contain Fe ions (Mn ferrites, Ni ferrites and Zn ferrites), i.e., $E_a = 0.1$–0.5 eV [18], and that for the tetragonal Mn_3O_4 spinel, i.e., $E_a = 0.4$ eV [19].

4. Discussion

Now, we discuss the origin of the relationship between T_C and δ for the $LiMn_2O_{4-\delta}$ samples with $\delta \leqslant 0.1$. The average valence of the Mn ions in $LiMn_2O_{4-\delta}$ is expressed by $3.5 - \delta$; the ratio of the amounts of Mn^{3+} ions and Mn^{4+} ions, $[Mn^{3+}]/[Mn^{4+}]$, is represented as $(1+2\delta)/(1-2\delta)$. This means that $[Mn^{3+}] > [Mn^{4+}]$ in the oxygen deficient spinels, though $[Mn^{3+}] = [Mn^{4+}]$ in the stoichiometric compound. The electron configurations of Mn^{3+} and Mn^{4+} are represented as $t_{2g}3e_g^1$ and $t_{2g}3e_g^0$, respectively. Since the former configuration is in a high-spin state, Mn^{3+} ions at the octahedral site give tetragonal distortions due to a Jahn–Teller effect. At that time, it is favourable to distort the nearest-neighbouring MnO_6 octahedra in the same fashion; that is, the directions of elongation and shrinkage of one MnO_6 octahedron coincide with those of adjacent MnO_6 octahedron [20]. This is because the Jahn–Teller distortions do not interfere with each other in such a configuration of the MnO_6 octahedra. Therefore, the increase in the amount of Mn^{3+} ions in $LiMn_2O_{4-\delta}$ induces a cooperative Jahn–Teller distortion between the MnO_6 octahedra; as a result, $LiMn_2O_{4-\delta}$ undergoes the phase transition from cubic to tetragonal phase. Indeed, the tetragonal phase is stable in $LiMn_2O_{3.90}$ even at ambient temperature [12]. Consequently, one may expect

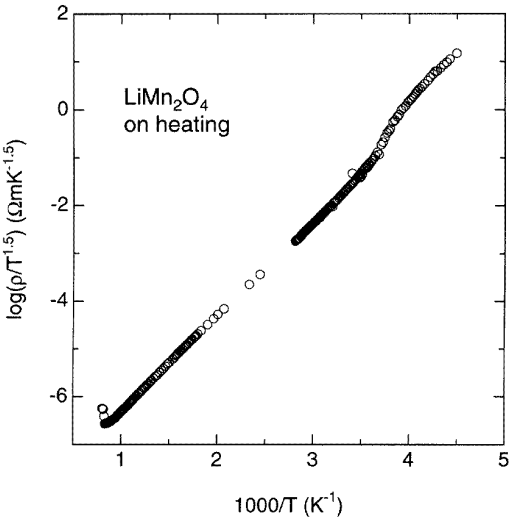

Figure 9. The relationship between $\log(\rho/T^{1.5})$ and T^{-1} for $LiMn_2O_4$; where ρ is the resistivity.

that the magnitude of T_C increases with increasing δ up to 0.1. Nevertheless, as seen in figure 2, the T_C-against-δ curve was found to exhibit a broad minimum at around $\delta = 0.05$. In order to solve this puzzle, we have to look for the effect which reduces T_C, that is, we assume that the dependence of T_C on δ is explained using a competition between two effects; one raises T_C and another reduces T_C. Here, we employ the following two mechanisms for reducing T_C; (i) dilution of the nearest-neighbour interaction and (ii) delocalization of the e_g electron.

4.1. Dilution of the nearest-neighbour interaction

For the oxygen deficient spinels $LiMn_2O_{4-\delta}$, two neighbouring Mn ions cannot overlap without the intervening O; in consequence, the interaction between two neighbouring Mn ions is expected to weaken with increasing δ. In order to estimate the effect of oxygen deficiency on the magnitude of T_C, we employ the model for the spinels proposed by Wojtowicz [20]. According to his work, for the spinels having the formula $A[B_{1-x}C_x]_2O_4$, where the B ions give Jahn–Teller distortions in the octahedral sites, while the C ions remain the regular octahedra, the relationship between T_C and x is simply given by

$$T_C(x) = (1 - x)T_C(0) \tag{1}$$

where $T_C(0)$ is the temperature of the transition from cubic to tetragonal phases for the pure material. In the $A[B_{1-x}C_x]_2O_4$ spinels, the C ions act to dilute the nearest-neighbour interaction between the B ions. Assuming that the oxygen deficiency plays a similar role to that of the C ions, we obtain $T_{C,calc}(0.026) = 239$ K for $LiMn_2O_{3.974}$ using the value of $T_C(0) = 245$ K and $x = \delta = 0.026$. This value is comparable with the magnitude of T_C measured for $LiMn_2O_{3.974}$, i.e., $T_C(0.026) = 241 \pm 1$ K; the discrepancy between the two values is explained as follows.

(i) Making a comparison with the case of the $A[B_{1-x}C_x]_2O_4$ spinels, the interaction between the B ions is not so affected by the oxygen deficiency. Since the connection of the BO_6 octahedra is characterized as edge sharing, there are two intervening O ions between two neighbouring Mn ions. Thus, the effect of δ on T_C could be roughly estimated to be half of that of the C ions; if so, we obtain $T_{C,calc}(0.026) = 242$ K, and this value seems to be in good agreement with the experimental result.

(ii) As mentioned above, $[Mn^{3+}]$ increases with increasing δ in $LiMn_2O_{4-\delta}$; hence, the magnitude of T_C also increases with increasing δ. As a result, the decrease in T_C is rather small compared with the value obtained by (1).

In order to further understand the mechanism of the phase transition in $LiMn_2O_{4-\delta}$, precise structural analyses for $LiMn_2O_{4-\delta}$ should be carried out with respect to temperature and δ at temperatures above and below T_C.

4.2. Delocalization of the e_g electron

The $La_{1-x}Sr_xMnO_3$ perovskites are known to be an antiferromagnetic insulators, associated with the cooperative Jahn–Teller distortions due to Mn^{3+} ions in a high-spin state. However, for $La_{1-x}Sr_xMnO_3$ with $x \geqslant 0.2$, metallic conductivity occurs and the cooperative Jahn–Teller distortion disappears. This is because the e_g electron is delocalized due to a doping of Sr^{2+} ions [21]. In $LiMn_2O_4$ spinel, the oxygen forms a 90° bridge between two Mn ions, while the oxygen forms a 180° bridge between two Mn ions in $LaMnO_3$ perovskite. Therefore, two neighbouring Mn ions in $LiMn_2O_4$ cannot overlap with the same p orbital of their binding O [22]. As a result, the interaction between Mn ions is considered to be too weak to give an itinerant-electron bandwidth [23]; thus, $LiMn_2O_4$ is known to be a small polaron semiconductor, as seen in figure 9.

Nevertheless, we may assume that the delocalized e_g electron is also generated due to the oxygen deficiency of $LiMn_2O_{4-\delta}$. Indeed, as seen in figure 8, resistivity of $LiMn_2O_{3.899}$ decreases by about one order of magnitude compared with that of $LiMn_2O_4$ at 250 K. However, at ambient temperature, ρ of every sample appeared to be $\sim 200\ \Omega$ m. Furthermore, the oxygen deficiency induced the increase in ρ at around 1200 K (see figure 9). Therefore, at present, this assumption is unlikely for the mechanism of the reduction in T_C.

5. Summary

We have investigated the effect of oxygen deficiency on the phase transition from cubic to tetragonal phase by measurements of differential scanning calorimetry (DSC), magnetic susceptibility (χ), ^{7}Li nuclear magnetic resonance (^{7}Li NMR) and electronic resistivity (ρ) for the $LiMn_2O_{4-\delta}$ spinels with $\delta = 0$–0.1. According to the DSC analysis, the transition temperature for a stoichiometric compound (T_C) is determined to be 245 ± 1 K with a thermal hysteresis of 5 ± 2 K. As δ increases from 0 to 0.066, the magnitude of T_C is found to decrease by about 4 K; then, the magnitude of T_C increases rapidly with further increasing of δ up to 0.10; thus, the T_C-versus-δ curve seems to exhibit a broad minimum at around $\delta = 0.05$. This result is supported by the measurements of χ, ^{7}Li NMR and ρ. As δ increases from zero, the average valence of the Mn ions reduces from +3.5 in proportion to δ; on the other hand, the interaction between two neighbouring Mn ions is diluted. The former effect raises T_C, whereas the latter reduces it. Therefore, the dependence of T_C on δ is explained qualitatively using competition between the two effects. For the samples with $\delta = 0.026$, we can obtain $T_{C,calc}(0.026) = 242$ K using a modified model as proposed by Wojtowicz; this value seems to be in good agreement with the experimental result.

Acknowledgments

We would like to thank Ms A Takagi of Toyota CRD Laboratories for her help in DSC measurements.

References

[1] Thackeray M M, David W I F, Bruce P G and Goodenough J B 1983 *Mater. Res. Bull.* **18** 461
[2] Scrosati B 1992 *J. Electrochem. Soc.* **139** 2776 and references therein
[3] Ohzuku T 1994 *Lithium Batteries* ed G Pistoia (Amsterdam: Elsevier) pp 239–80 and references therein
[4] Hunter J C 1981 *J. Solid State Chem.* **39** 142
[5] David W I F, Thackeray M M, Bruce P G and Goodenough J B 1984 *Mater. Res. Bull.* **19** 99
[6] 1986 *Joint Committee on Powder Diffraction Standards* (International Center for Diffraction Data, Swarthmore) No. 35–782
[7] Yamada A and Tanaka M 1995 *Mater. Res. Bull.* **30** 715
[8] Sugiyama J, Tamura T and Yamauchi H 1995 *J. Phys.: Condens. Matter* **7** 9755
[9] Tarascon J M, Wang E, Shokoohi F K, McKinnon W R and Colson S 1991 *J. Electrochem. Soc.* **138** 2859
[10] Tarascon J M, McKinnon W R, Coowar F, Bowmer T N, Amatucci G and Guyomard D 1994 *J. Electrochem. Soc.* **141** 1421
[11] Yamada A, Miura K, Hinokuma K and Tanaka M 1995 *J. Electrochem. Soc.* **142** 2149
[12] Sugiyama J, Atsumi T, Hioki T, Noda S and Kamegashira N 1996 *J. Alloys Compounds* **235** 163
[13] Englman R and Halperin B 1970 *Phys. Rev.* B **2** 75 and references therein
[14] Sugiyama J, Hioki T, Noda S and Kontani M 1996 unpublished
[15] Kaplan M D and Vekhter B G 1995 *Cooperative Phenomena in Jahn–Teller Crystals* (New York: Plenum) and references therein
[16] Morgan K R, Collier S, Burns G and Ooi K 1994 *J. Chem. Soc. Chem. Commun.* 1719
[17] Kumagai N, Fujiwara T, Kumagai N, Binda T, Tannno K and Horiba T 1994 *Proc. 2nd. Int. Symp. on Ionic and Mixed Conducting Ceramics* pp. 514–31
[18] Smit J and Wijn H P J 1959 *Ferrites* (New York: Wiley) and references therein
[19] Fine M E and Chiou C 1957 *Phys. Rev.* **105** 121
[20] Wojtowicz P J 1959 *Phys. Rev.* **116** 32
[21] Goodenough J B 1971 *Prog. Solid State Chem.* **5** 145 and references therein
[22] Goodenough J B 1963 *Magnetism and the Chemical Bond* (New York: Wiley) and references therein
[23] Goodenough J B, Manthiram A and Wnetrzewski B 1993 *J. Power Sources* **43–4** 269